System size dependence of strange particle yields and spectra at $\sqrt{s_{NN}} = 17.3$ GeV

Ingrid Kraus for the NA49 Collaboration
Gesellschaft für Schwerionenforschung (GSI), Darmstadt, Germany

Abstract. Yields and spectra of strange hadrons (K^+, K^-, ϕ, Λ and $\bar{\Lambda}$) as well as of charged pions were measured in near central C+C and Si+Si collisions at 158 A GeV beam energy with the NA49 detector. Together with earlier data for p+p, S+S and Pb+Pb reactions the system size dependence can be studied. Relative strangeness production rises fast and saturates at about 60 participating nucleons; the net hyperon spectra show an increasing shift towards midrapidity for larger colliding nuclei. An interpretation based on the formation of coherent systems of increasing volume is proposed. The transverse mass spectra can be described by a blast wave ansatz. Increasing flow velocity is accompanied by decreasing temperatures for both kinetic and chemical freeze out. The increasing gap between inelastic and elastic decoupling leaves space for rescattering.

PACS numbers: 25.75.-q

1. Introduction

The production of strange particles in heavy ion collisions is studied in many experiments since it had been proposed as a signature for the transition to a deconfined state of strongly interacting matter [1]. Although enhanced strangeness production in A+A collisions relative to elementary reactions is observed over a wide range of c.m. energy [2], the question about its origin is still unsolved. This motivated the systematic study of symmetric collisions of nuclei with increasing mass number A.

The presented data were recorded with the NA49 hadron spectrometer [3] at the CERN SPS. The analysis of meson ($\pi^{\pm}$, $K^{\pm}$, ϕ) and Λ hyperon production is described in [4], the preliminary results for $\bar{\Lambda}$ baryons were obtained analogously.

2. Results

The yields of all particles under study were measured in (y,p_T) bins, the transverse mass ($m_T = \sqrt{m_0^2 + p_T^2}$) spectra at midrapidity are shown in figure 1 (left). Fits with the thermal ansatz

$$\frac{1}{m_T} \cdot \frac{\mathrm{d}^2 n}{\mathrm{d}y \cdot \mathrm{d}m_T} = \mathrm{c} \cdot \mathrm{e}^{-m_T/T} \qquad (1)$$

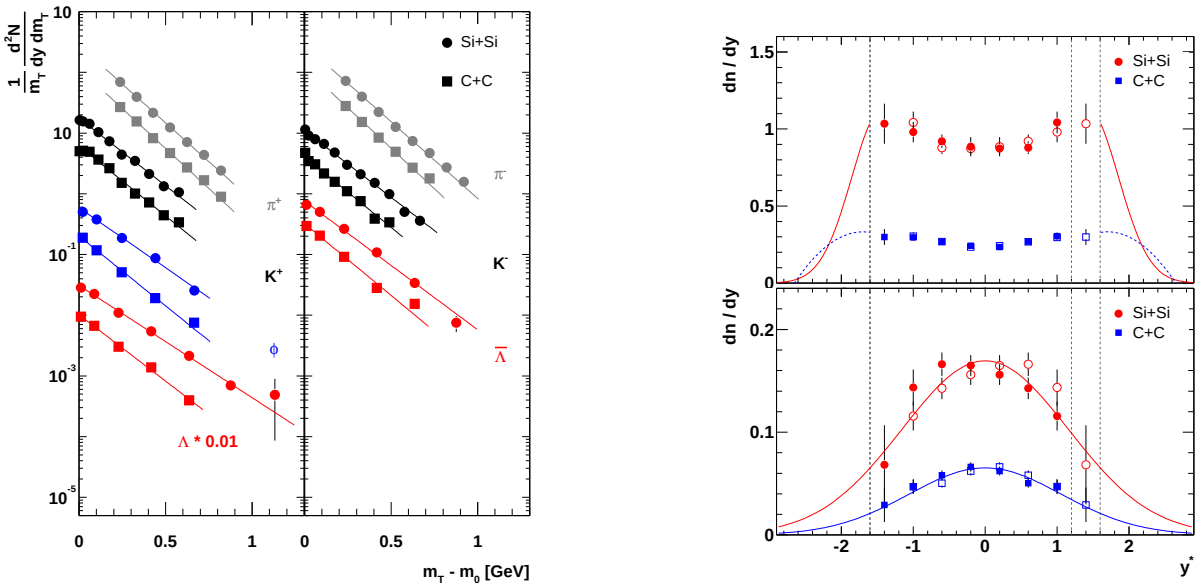

Figure 1. Left: transverse mass spectra of various particles, measured at midrapidity in C+C (■) and Si+Si (●) reactions. Shown are the exponential fits with equation 1. Right: rapidity spectra of Λ (top) and $\bar{\Lambda}$ hyperons (bottom, preliminary). Only statistical errors are included.

were used to extrapolate to p_T regions not covered by the measurement. The rapidity densities $\mathrm{d}n/\mathrm{d}y$ of the hyperons are shown in figure 1 (right), while the mesons are presented in [4]. For the extrapolation to the very forward region the pion rapidity distributions were approximated by a superposition of two Gaussians displaced symmetrically around midrapidity, whereas single Gaussians were used for the other mesons and $\bar{\Lambda}$ hyperons. To obtain the yields of Λ hyperons their rapidity distributions were extrapolated by shapes adopted from p+p and S+S measurements. The mean of both approximations was taken for C+C, the shape from S+S was used for Si+Si (lines in figure 1).

3. Discussion

3.1. Strange particle production

The strange particle yield per pion is shown in figure 2 together with data from p+p and Pb+Pb collisions [5] measured by the NA49 Collaboration and S+S results [6] from NA35. All presented data on pions and hyperons are corrected for feed down contaminations. The mean number of nucleons in the geometrical overlap area $\langle N_W \rangle$ serves as a measure of the system size. The ratio of strange hadrons to pions exhibits for all considered particles a fast rise in small systems and reaches the level of Pb+Pb interactions at about 60 wounded nucleons.

Empirical scaling parameters as e.g. the nucleon or collision density [7] suggest that the density reached in A+A interactions has an impact on the strangeness production.

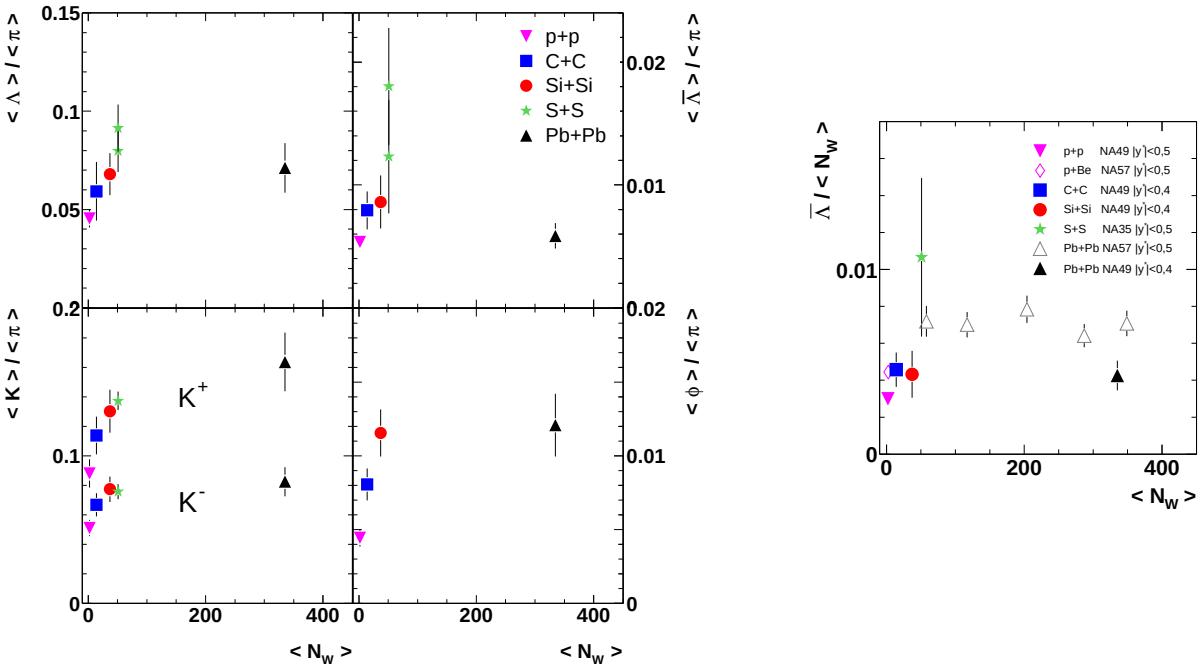

Figure 2. Left: multiplicity of hyperons, charged kaons and ϕ mesons per pion, $\langle\pi\rangle = \frac{1}{2}\big(\langle\pi^+\rangle + \langle\pi^-\rangle\big)$. Right: $\bar{\Lambda}$ density at midrapidity per wounded nucleon in p+p (▼), p+Be (◊), C+C (■), Si+Si (●), minimum bias (△) and central Pb+Pb (▲) collisions at 158 A GeV as well as in S+S reactions (★) at 200 A GeV . The error bars represent the squared sum of statistical and systematic errors.

At sufficiently high density one might expect that the subsequent collisions do not occur independently anymore, but that connected domains of overlapping resonances or strings are created. These volumes can become quantum-mechanically coherent and decay as objects which can be considerably larger than those created in isolated p+p interactions.

The volume dependence of strangeness production is described in statistical models by the transition from canonical to grand canonical ensembles. The calculation by Tounsi and Redlich [8] agrees qualitatively with the measurements presented in figure 2, but quantitatively the saturation level is reached for a distinctly smaller number of participants in the model. Theory and experiment might be reconciled by two plausible modifications: assuming that only parts of the reaction volume that is spread over about 3 units of rapidity [9] are coherent or that the linear relationship between volume and number of participants used to link model and measurement has to be refined.

3.2. Chemical freeze out conditions

The measured particle yields can be reproduced by the statistical hadronisation model of Becattini [10], see figure 3. The strangeness production in the corresponding equilibrated resonance gas is suppressed ($\gamma_S < 1$). This suppression diminishes with increasing system size (figure 4), following the observed strangeness enhancement. The

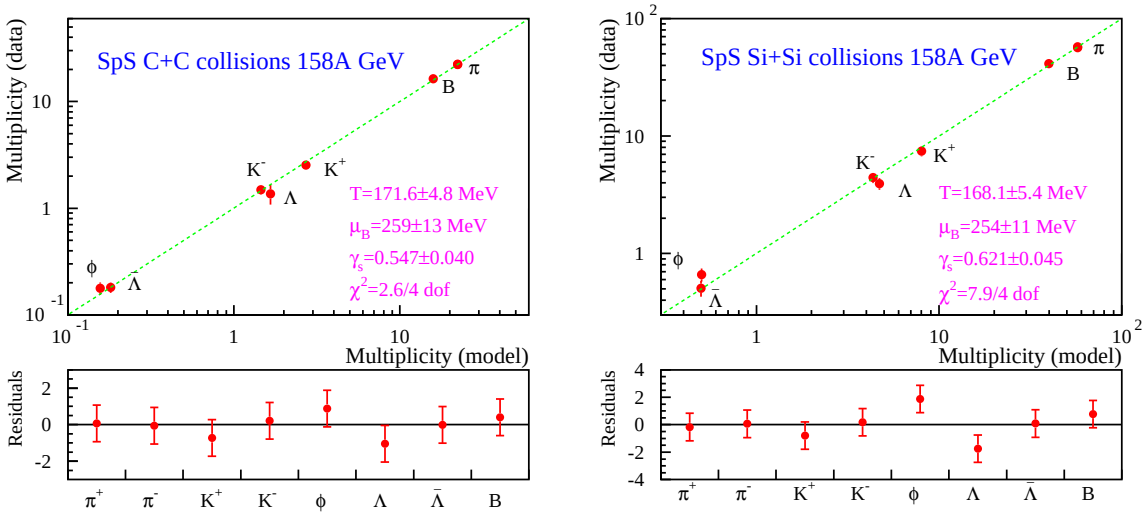

Figure 3. Comparison of the measured preliminary particle yields in C+C (left) and Si+Si collisions (right) to calculations with the statistical hadronisation model [10].

baryochemical potential μ_B does not depend significantly on the system size, while the decoupling temperature T_{ch} is higher in smaller reaction volumes. This would leave less room for inelastic rescattering in the small systems, if the varying T_{ch} is not entirely provoked by the changing γ_S as suggested in [14]. The freeze out points of C+C and Si+Si reactions appear in the QCD phase diagram in the vicinity of the phase boundary as seen in figure 4.

3.3. Absorption of $\bar{\Lambda}$ *hyperons*

The increasing absorption of anti-baryons ($\bar{p}$ and $\bar{d}$) with increasing centrality of Pb+Pb reactions at 158 A GeV was observed in a forward rapidity window (y = 3.7) by the NA52 Collaboration [23] and explained with an increasing baryochemical potential. In contrast to that, the $\langle\bar{\Lambda}\rangle$ yield per pion in central Pb+Pb collisions is not significantly smaller than in Si+Si reactions (figure 2 left), while the midrapidity densities are on the same level. Moreover the measurement by the NA57 Collaboration [24] indicates even a further increase from central Si+Si to Pb+Pb data at different centralities (figure 2 right). This is in accord with the almost constant μ_B shown in figure 4.

3.4. Particle ratios

Both, the $\langle \mathrm{K}^- \rangle / \langle \mathrm{K}^+ \rangle$ as well as the $\langle\bar{\Lambda}\rangle$ /$\langle\Lambda\rangle$ ratio (figure 5) of the total yields exhibit no significant dependence on the system size. Due to that, the strange hadron potential μ_S calculated (with the strange quark potential μ_s) as [25]

$$\mu_S = \frac{1}{3}\,\mu_B - \mu_s \qquad \text{with} \qquad \frac{\langle\Lambda\rangle}{\langle\bar{\Lambda}\rangle} \cdot \left(\frac{\langle K^-\rangle}{\langle K^+\rangle}\right)^2 = \exp\left(6 \cdot \frac{\mu_s}{T}\right) \qquad (2)$$

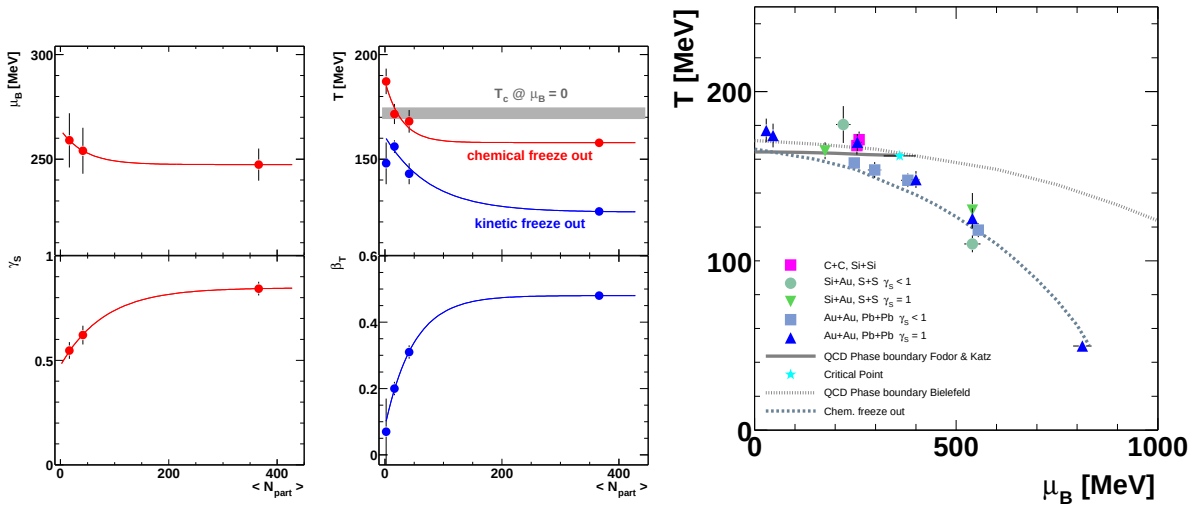

Figure 4. Left: chemical freeze out conditions for C+C, Si+Si, Pb+Pb at 158 A GeV from fits with the statistical hadronisation model [10, 11]. The curves are shown to guide the eye and represent a functional form $f(\langle N_{part}\rangle) = a + b \cdot \exp\,(c \cdot \langle N_{part}\rangle)$. Middle: freeze out conditions for p+p, C+C, Si+Si, Pb+Pb at 158 A GeV. The temperatures at chemical decoupling are from fits with the statistical hadronisation model [10, 11]. The kinetic freeze out temperature and the transverse flow velocity β_T are from blast wave fits to the transverse mass spectra, equation 3. The values for p+p and Pb+Pb interaction were taken from [12]. The critical temperature T_c is from lattice QCD calculations [13].
Right: QCD phase diagram. The phase boundary between deconfined and hadronic matter was estimated with lattice calculations by the Bielefeld [15] as well as by the Budapest group [16]. The parametrisation of the chemical freeze out points as a curve of constant energy per hadron of $\langle E\rangle/\langle N\rangle = 1$ GeV is taken from [17]. The C+C and Si+Si data [10] lie between the Si+Au measurements at the AGS at 14.6 A GeV and the S+S data at 200 A GeV. Model calculations with $\gamma_S = 1$ are from [18], those with free γ_S are from [19]. The freeze out points determined from the fits to the Au+Au and Pb+Pb data with $\gamma_S = 1$ from SIS [20], AGS [18] and SPS [21] up to RHIC energies [22] agree with those from the fits with free γ_S for the AGS and SPS [11].

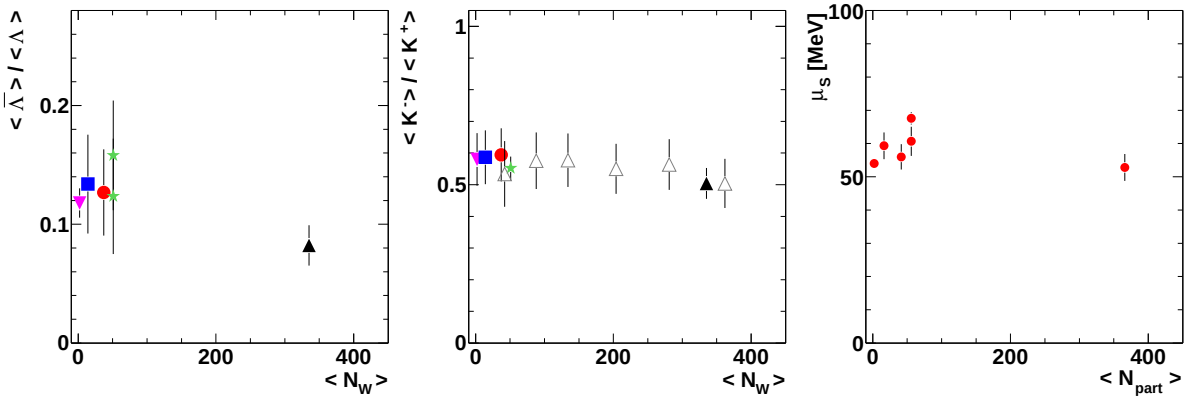

Figure 5. $\langle\bar{\Lambda}\rangle/\langle\Lambda\rangle$ (left) and $\langle K^-\rangle/\langle K^+\rangle$ ratio (middle) of the total yields measured in p+p (▼), C+C (■), Si+Si (●), minimum bias (△) and central Pb+Pb (▲) collisions at 158 A GeV as well as in S+S reactions (★) at 200 A GeV. The error bars represent the squared sum of statistical and systematic errors. The strange hadron potential μ_S (right) is calculated from these ratios.

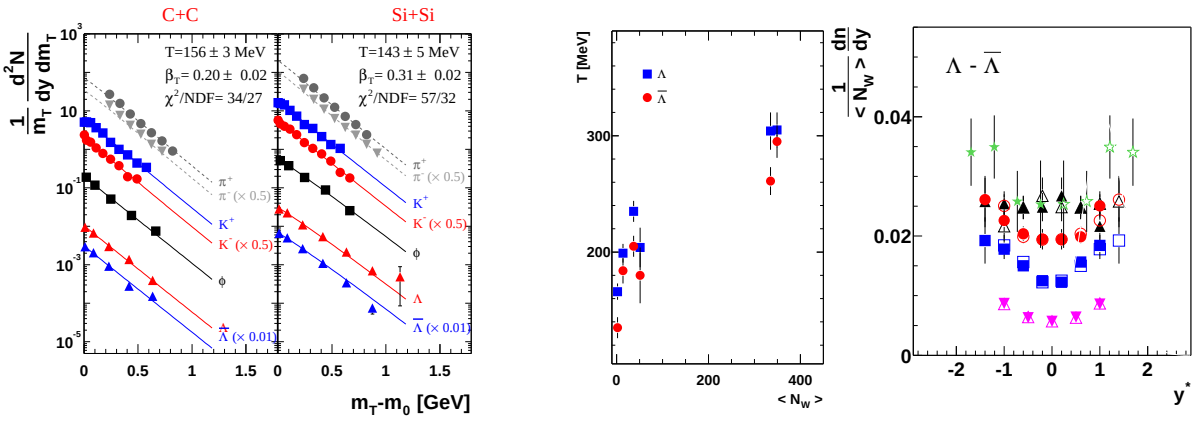

Figure 6. Left: transverse mass spectra of various particles from C+C (left part) and Si+Si collisions (right part) measured at midrapidity. Also shown are the fits with the blast wave model (equation 3).
Middle: Inverse slope parameters of Λ (■) and $\bar{\Lambda}$ (●) hyperons (equation 1) in p+p, C+C, Si+Si, S+S and Pb+Pb collisions.
Right: net hyperon rapidity density normalised to the number of wounded nucleons $\langle N_W \rangle$ measured in p+p (▼), C+C (■), Si+Si (●) and Pb+Pb (▲) collisions at 158 A GeV as well as in S+S reactions (★) at 200 A GeV. Only statistical errors are included.

is constant as well. In spite of zero net strangeness the potential is not vanishing, it amounts to about 60 MeV (figure 5). This is in agreement with the statistical model prediction [26] for the fitted values of T_{ch} and μ_B.

3.5. Net hyperon density

The $\bar{\Lambda}/\Lambda$ ratio at midrapidity (not shown) is (in contrast to the flat $\langle\bar{\Lambda}\rangle/\langle\Lambda\rangle$ ratio) steeply decreasing with increasing system size for small reaction volumes, followed by a saturation above about 60 wounded nucleons. The ratio reflects directly the changing Λ rapidity distribution while the shape of the $\bar{\Lambda}$ hyperon spectra remains the same. The difference of the two distributions, the net hyperon density, is shown in figure 6. The flattening of the $(\Lambda - \bar{\Lambda})$ rapidity spectra with increasing system size can be understood in terms of stronger stopping due to an increasing number of collisions. This leads to a successive shift of the incoming baryons from beam towards mid rapidity. Thereby the energy per nucleon deposited in the fireball is increasing and more energy for the excitation of resonances or strings is provided.

3.6. Transverse mass spectra

The inverse slope parameters T from exponential fits to the m_T spectra with equation 1 are systematically higher for Λ than for $\bar{\Lambda}$ hyperons as can be seen from figure 6. In small systems this may be traced back to the anti-correlation of the (higher $\bar{\Lambda}$) production threshold on one hand and the kinetic energy of the created particles on the other hand due to energy conservation [27]. The cause in the large systems is not clear.

The slopes of both, Λ and $\bar{\Lambda}$ hyperons, fit into the picture of growing radial flow with increasing system size. Moreover the m_T spectra can be approximated with a hydrodynamical model; here a simplified version from Schnedermann et al. [28] with constant flow velocity β_T is utilised to fit all particles except the pions simultaneously with the function

$$\frac{\mathrm{d}n}{m_T \cdot \mathrm{d}m_T} \propto m_T \cdot \mathrm{I}_0\left(\frac{p_T \cdot \sinh\rho}{T}\right) \cdot \mathrm{K}_1\left(\frac{m_T \cdot \cosh\rho}{T}\right), \tag{3}$$

where I_0 and K_1 are modified Bessel functions and ρ includes β_T: $\rho = \mathrm{atanh}\,\beta_T$. The fit to the C+C and Si+Si data is shown in figure 6, while the system size dependence of the kinetic freeze out temperature and flow velocity β_T is displayed in figure 4. The p+p and Pb+Pb spectra were fitted with the same formula. In p+p reactions β_T is compatible with zero; in larger systems β_T steeply increases. The increasing radial flow is accompanied by a decreasing kinetic freeze out temperature; T_{kin} drops by 30 MeV between C+C and Pb+Pb collisions. Thereby the gap between chemical and thermal decoupling temperatures $\Delta\, T$ increases with size of the colliding nuclei, so more rescattering is expected in the larger systems.
The largest $\Delta\, T$ is observed in p+p interactions, where neither rescattering nor flow is expected. This questions the mechanism described above as the only source of the effect. The broadening of p_T spectra is already seen in p+A data and multiple scattering is given there as an alternative explanation [29]. Furthermore there are models which describe the measured yields and spectra reasonably well by a single freeze out, e.g. [30].

4. Summary

Yields and spectra of strange hadrons and charged pions in p+p, C+C, Si+Si, S+S and Pb+Pb collisions were presented. The fast rise of the relative strangeness production, followed by a saturation above about 60 participating nucleons, together with the increasing shift of net hyperons towards mid rapidity with increasing size of the colliding nuclei suggests the creation of coherent domains as a possible interpretation. The hadronisation of the small systems occurs in the vicinity of the phase boundary. No significant absorption of $\bar{\Lambda}$ hyperons is seen. The transverse mass spectra can be described by a blast wave ansatz. Fits to the data indicate increasing flow velocity accompanied by decreasing temperatures for both kinetic and chemical freeze out. The increasing gap between inelastic and elastic decoupling in A+A collisions leaves space for rescattering.

[1] Rafelski J and Müller B 1982 *Phys. Rev. Lett.* **48** 1066
Koch P, Müller B and Rafelski J 1986 *Phys. Rep.* **142** 167
[2] Ritter H G and Wang X (editors) 2004 *Quark Matter 2004* (Institute of Physics Publishing)
[3] Afanasiev S V *et al* (NA49 Collaboration) 1999 *Nucl. Instr. Meth.* A **430** 210
[4] Alt C *et al* (NA49 Collaboration) *Preprint* nucl-ex/0406031

[5] Sikler F *et al* (NA49 Collaboration) 1999 *Nucl. Phys.* A **661** 45c
Afanasiev S V *et al* (NA49 Collaboration) 2000 *Phys. Lett.* B **491** 59
Afanasiev S V *et al* (NA49 Collaboration) 2002 *Phys. Rev.* C **66** 054902
Susa T *et al* (NA49 Collaboration) 2002 *Nucl. Phys.* A **698** 491c
Barna D 2002 *Ph.D. thesis, University of Budapest*
Höhne C 2003 *Ph.D. thesis, University of Marburg* http://archiv.ub.uni-marburg.de/diss/-z2003/0627/
Anticic T *et al* (NA49 Collaboration) 2004 *Phys. Rev. Lett.* **93** 022302
[6] Bartke J *et al* (NA35 Collaboration) 1990 *Z. Phys.* C **48** 191
Bächler J *et al* (NA35 Collaboration) 1993 *Z. Phys.* C **58** 367
Alber T *et al* (NA35 Collaboration) 1994 *Z. Phys.* C **64** 195
Alber T *et al* (NA35 Collaboration) *Preprint* hep-ex/9711001
[7] Bialkowska H and Retyk W 2001 *J. Phys.* G **27** 397
Höhne C *et al* (NA49 Collaboration) 2003 *Nucl. Phys.* A **715** 474c
[8] Tounsi A and Redlich K 2002 *J. Phys.* G **28** 2095
[9] Appelshäuser H. *et al* (NA49 Collaboration) 1999 *Phys. Rev. Lett.* **82** 2471
[10] Becattini F 2004 *private communication*
[11] Becattini F *et al* 2004 *Phys. Rev.* C **69** 024905
[12] van Leeuwen M *et al* (NA49 Collaboration) 2003 *Nucl. Phys.* A **715** 161c
van Leeuwen M 2004 *private communication*
[13] Fodor Z and Katz S D 2002 *JHEP 0203* 014 (*Preprint* hep-lat/ 0106002)
[14] Cleymans *et al Preprint* hep-ph/0409071
[15] Allton C R *et al* 2002 *Phys. Rev.* D **66** 074507
[16] Fodor Z and Katz S D *Preprint* hep-lat/0402006
[17] Cleymans J and Redlich K 1998 *Phys. Rev. Lett.* **81** 5284
[18] Braun-Munzinger P *et al* 1996 *Phys. Lett.* B **365** 1
Braun-Munzinger P *et al* 1995 *Phys. Lett.* B **344** 43
[19] Becattini F *et al* 1998 *Eur. Phys. J.* C **5** 143
Cleymans J *et al* 1997 *Z. Phys.* C **74** 319
[20] Becattini F *et al* 2001 *Phys. Rev.* C **64** 024901
[21] Braun-Munzinger P, Heppe I and Stachel J 1999 *Phys. Lett.* B **465** 19
[22] Braun-Munzinger P *et al* 2001 *Phys. Lett.* B **518** 41
[23] Ambrosini G *et al* (NA52 Collaboration) 1999 *New J. Phys.* **1** 22.1
[24] Bruno G E *et al* (NA57 Collaboration) 2004 *J. Phys.* G **30** S717
[25] Sollfrank J *et al* 1994 *Z. Phys.* C **61** 659
[26] Braun-Munzinger P, Redlich K and Stachel J, *Preprint* nucl-th/ 0304013 to appear in *Quark Gluon Plasma 3*, eds. R.C. Hwa and X.N. Wang, World Scientific Publishing
[27] Kafka T *et al* 1977 *Phys. Rev.* D **16** 1261
[28] Schnedermann E and Heinz U 1994 *Phys. Rev.* C **50** 1675
[29] Fischer H G *et al* (NA49 Collaboration) 2003 *Nucl. Phys.* A **715** 118c
[30] Letessier J *et al* 2001 *J. Phys.* G **27** 427
Broniowski W and Florkowski W 2002 *Phys. Rev. Lett.* **87** 272302